

LIRIS multi-slit H α spectroscopy of a $z \sim 1$ DEEP2 sample of star-forming galaxies

Nayra Rodríguez-Eugenio¹, Kai G. Noeske², Jose Acosta-Pulido¹, Rafael Barrena¹, Francisco Prada³, Arturo Manchado^{1,4} and EGS Teams

Abstract. We present preliminary results of H α near-infrared spectroscopy of six galaxies with redshifts $z \sim 1$ drawn from the DEEP2 Galaxy Redshift Survey. The spectra have been taken with the multi-slit mode of LIRIS (Long-slit Intermediate Resolution Infrared Spectrograph) installed at the 4.2-m William Herschel Telescope. This is a pilot study for a larger program to obtain H α luminosities of about 50 star-forming galaxies at $z \sim 1$, with the aim of deriving the corresponding star formation rates (SFRs) from H α as well as studying the relationship with other SFR indicators. The new galaxy sample will be selected from the Extended Groth Strip Survey, where galaxies will also have measures of stellar masses, reddening, far-IR data, and galaxy morphologies.

1. Introduction

Several diagnostic methods have been used to measure star formation rates (SFRs) in galaxies, of which some of the most extensive are the rest-frame ultraviolet (UV) continuum (1500-2800 Å), H α recombination line, [O II] λ 3727 forbidden line, and the far-IR luminosity. These various SFR indicators are differently affected by dust extinction and by metallicity effects, and they are related to the emission of different stellar populations, leading to discrepancies between the corresponding SFRs measurements even after extinction corrections. Therefore, in order to make a reliable study of the global star formation history of the Universe, it is necessary to use the same SFR tracer from low to high redshifts, or to have good calibrations between different indicators.

The H α luminosity is an excellent direct tracer of the “instantaneous” SFR, it is immune to metallicity effects, and dust obscuration affecting H α can be mitigated by reddening correction. H α has been a common SFR tracer in low- z surveys, but at moderate redshifts there are only small statistical galaxy samples with H α measurements (e.g. Glazebrook et al. 1999; Tresse et al. 2002; Erb et al. 2003; Doherty et al. 2004; Shapley et al. 2005). At $z > 0.6$ H α is redshifted into the near-IR (NIR), where the high sky background entails the need of large total exposure times to obtain good spectral data of faint objects. Only with the

¹Instituto de Astrofísica de Canarias, Vía Láctea, E-38205 La Laguna, Tenerife, Spain.

²Lick Observatory, University of California, 1156 High Street, Santa Cruz, CA 95064, USA.

³Instituto de Astrofísica de Andalucía (CSIC), E-18008 Granada, Spain.

⁴CSIC, Spain.

recent development of multi-object NIR spectrographs we are able to obtain H α spectra of a significant number of high- z galaxies in realistic observing periods.

The goals of the LIRIS-EGS project are to probe the star formation history of the Universe at $z \sim 1$ using H α luminosities as SFR indicators, to obtain self-consistent redshift-one SFR calibrations between H α and other star formation tracers, and to complete this study with galaxy stellar masses, morphologies, metallicities and reddening estimations.¹ This project is possible thanks to the multi-slit mode of the NIR spectrograph LIRIS (Long-slit Intermediate Resolution Infrared Spectrograph), which allows simultaneous observations of about 15 galaxies, and thanks to the collaboration with the EGS teams. In this work we present the results of a pilot study where we wanted to probe the multi-slit capabilities of LIRIS at the 4.2-m William Herschel Telescope (WHT) to study the SFR properties of galaxies at $z \sim 1$ from H α spectroscopy. The cosmology $\Omega_M = 0.3$, $\Omega_\Lambda = 0.7$, $H_0 = 70 \text{ km s}^{-1} \text{ Mpc}^{-1}$ is assumed throughout.

2. Target Selection, Observations and Data Reduction

The sample of galaxies was drawn from the DEEP2 Redshift Survey (Davis et al. 2003), and they are objects for which we expected to find H α emission in the J-band, inferred from the presence of [O II] in emission in the DEEP2 Keck optical spectra. We pre-selected galaxies with redshifts in the range $0.8 \lesssim z \lesssim 1.3$ such that H α will appear in regions of good atmospheric transmission, with good quality of the redshift estimations (90% reliable), and with [O II] $\lambda 3727$ rest-frame equivalent widths larger than 20 Å. We did not apply a selection criterion based on OH sky lines to study how the presence of these lines near H α affects its detection. The final selection consists of six DEEP2 $z \sim 1$ galaxy targets within the $4.2 \times 4.2 \text{ arcmin}^2$ LIRIS field of view centred at RA=16^h47^m39^s.6, Dec=34°43'48''(J2000). The LIRIS multi-slit mask designed to observe these objects also includes holes for two acquisition stars.

The spectroscopic observations were carried out on 2005 June 22 with the multi-object mode of LIRIS at the 4.2-m WHT. LIRIS is a NIR (0.9-2.4 μm) intermediate resolution spectrograph, with a Hawaii-II detector cooled at $\sim 70 \text{ K}$, and a pixel scale of 0.25 arcsec (Manchado et al. 2000). We used a zJ grism and a slit width of 0.9 arcsec, yielding a dispersion of 6 Å per pixel, and a resolution $\lambda/\Delta\lambda \sim 600$. During the observations the telescope was nodded between three positions along the slit, with a separation of 4 arcsec between contiguous positions. The total exposure time was 3.5 hours divided into 7 series of three 600 sec exposures, ensuring that we are limited by photon noise.

Our spectroscopic reduction includes a first order “extra-sky subtraction” process, and wavelength and flux calibration. No dark or flat-field corrections were performed. In the first case the reason is the low temperature of the LIRIS detector, while the second decision was made on the basis of the noisier results found after this correction, due to the absence of continuum in the galaxy spectra. The reduced emission line spectra are shown in Figure 1. We measured the H α integrated fluxes, associated errors, and FWHMs, by interactively fitting

¹This research is partly funded by the Spanish Min. de Educacion y Ciencia (AYA2004-03136).

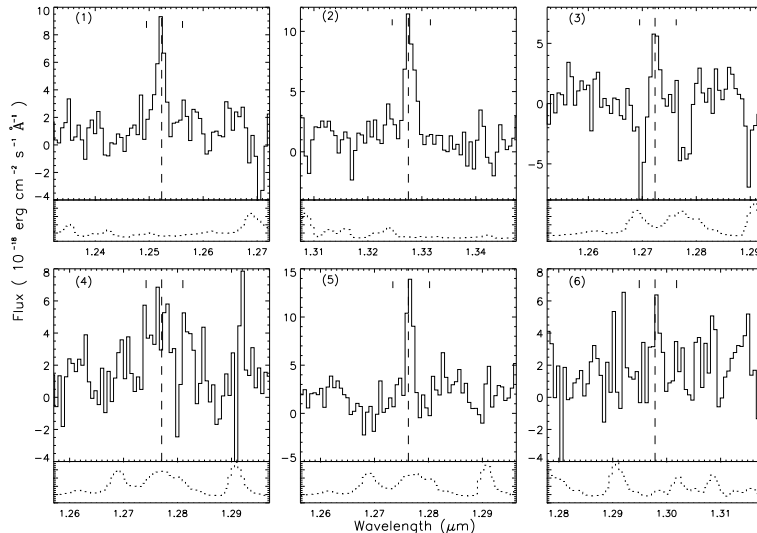


Figure 1. Observed-frame spectra of our six LIRIS/DEEP2 galaxies. The expected position for $H\alpha$ given the optical spectroscopic redshift is marked with a vertical dashed line, and the vertical bars to either side show the predicted positions of the $[N II]\lambda 6548$ and $[N II]\lambda 6583$ lines. Plotted below each galaxy spectrum is the subtracted night sky spectrum in arbitrary flux units. The OH sky lines are not resolved in these spectra.

Gaussian functions to the background-subtracted emission-line profiles using the package *fitlines* under IRAF (Acosta-Pulido 2000).

3. Preliminary Results and Discussion

We find four clear $H\alpha$ detections with $S/N > 4$ (galaxies 1, 2, 3 and 5), and another $3\text{-}\sigma$ detection (galaxy 6), out of the six observed galaxies. Only the two galaxies with $H\alpha$ emission away from sky lines have FWHMs greater than or similar to the instrumental resolution. This result highlights the importance of a target selection criterion based on the distance between $H\alpha$ and intense OH skylines, which has been included in the selection of the new LIRIS-EGS sample.

We obtained the $H\alpha$ luminosities, $L_{H\alpha}$, of the galaxies and derived SFRs using the Kennicutt (1998) conversion (2). As our galaxies have redshifts near unity, we directly derived UV luminosity densities, $L_\nu(2200 \text{ \AA})$, from the DEEP2 B magnitudes (AB) as a good first approximation. We also derived UV SFRs using the Kennicutt (1998) conversion (1). These magnitudes are summarized in Table 1 together with the DEEP2 identification numbers and redshifts (z_{opt}) of the galaxies, and redshifts derived from LIRIS $H\alpha$ detections ($z_{H\alpha}$). In Figure 2 we plot the $H\alpha$ versus UV luminosities of our galaxies and of three $z \sim 1$ DEEP2 galaxies from Shapley et al. (2005).

Our non-extinction corrected SFRs inferred from $H\alpha$ are smaller than the corresponding UV SFRs in all cases except one, and the same result is found for the Shapley et al. galaxies. Other studies of the UV - $H\alpha$ SFR relation

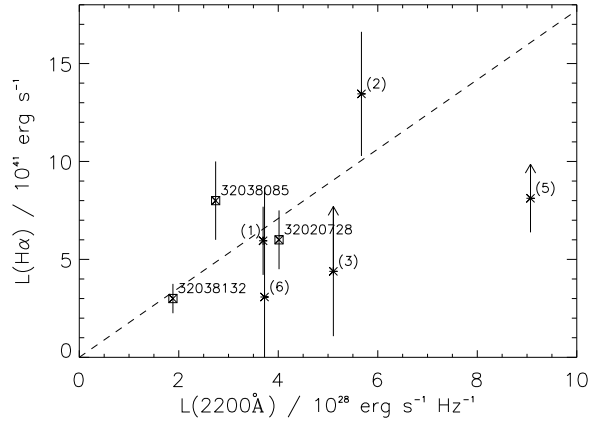


Figure 2. Comparison of the $H\alpha$ luminosity and the UV 2200Å flux for the individual galaxies. The dashed line represents the relation between L_ν and $L_{H\alpha}$ to yield the same SFR using the Kennicutt conversions. Starred symbols correspond to our galaxies and squares to the $z \sim 1$ galaxies from Shapley et al. (2005). Arrows in galaxies (3) and (5) show that these luminosities are lower limits due to subtraction of near intense sky lines.

(e.g. Glazebrook et al. 1999; Doherty et al. 2004) had found opposite results, with underestimations of the UV SFRs by a factor of 2 or 3 from not extinction-corrected data. One of the reasons for this discrepancy is that four of the $H\alpha$ lines in our spectra are affected by the subtraction of very intense OH sky lines, which could reduce the $H\alpha$ fluxes. Also, the galaxies appear to be extended in the I-band DEEP2 images, with a mean FWHM of 1.4 arcsec, so we need to apply aperture corrections to make up for our 0.9 arcsec wide slits.

Even though final results are not achieved, with this pilot study we have demonstrated that LIRIS is highly suitable for obtaining $H\alpha$ spectroscopy of a significant number of $z \sim 1$ star-forming galaxies. With the upcoming LIRIS-EGS sample we will have a comprehensive dataset that includes not only $H\alpha$ and UV continuum information, but also [O II] and far-IR luminosities, stellar masses, reddening estimations, galaxy morphologies and metallicities.

Table 1. Observed galaxy properties derived from DEEP2 and LIRIS data

id	DEEP2 id	z_{opt}	$z_{H\alpha}$	L_ν (2200 Å) (10^{28} erg s $^{-1}$ Hz $^{-1}$)	SFR $_{UV}$ (M_\odot yr $^{-1}$)	$L_{H\alpha}$ (10^{41} erg s $^{-1}$)	SFR $_{H\alpha}$ (M_\odot yr $^{-1}$)
1	21002068	0.90820	0.9079	3.69	5.2	5.95 ± 1.74	4.7 ± 1.4
2	21006790	1.02276	1.0231	5.67	7.9	13.45 ± 3.17	10.6 ± 2.5
3	21002050	0.93875	0.9388	5.11	7.1	4.39 ± 3.31	3.5 ± 2.6
4	21006616	0.94590	-	3.93	5.5	-	-
5	21006922	0.94472	0.9451	9.07	12.7	8.12 ± 1.74	6.4 ± 1.4
6	21006954	0.97758	0.9780	3.72	5.2	3.08 ± 5.60	2.4 ± 4.4

References

- Acosta-Pulido, J.A. 2000, ASP Conference Proceedings, 216, 663
Davis, M., Faber, S.M., Newman, J. et al. 2003, Proc. SPIE, 4834, 161
Doherty, M., Bunker, A., Sharp, R., Dalton, G., Parry, I., Lewis, I., et al. 2004, MNRAS, 354, L7
Erb, D.K., Shapley, A.E., & Steidel, C.C. 2003, ApJ, 591, 101
Glazebrook, K., Blake, C., Economu, F., Lilly, S., & Colless, M. 1999, MNRAS, 306, 843
Kennicutt, R.C. 1998, ARA&A, 36, 189
Manchado, A., Barreto, M., Acosta-Pulido, J.A., Prada, F., et al. 2000, Proc. SPIE, 4008, 1162
Shapley, A.E., Coil, A.L., & Ma, C.-P. 2005, ApJ, 635, 1006
Tresse, L., Maddox, S.J., Le Fèvre, O., & Cuby, J.G. 2002, MNRAS, 337, 369